Comparison of AASHTO Structural Evaluation Techniques Using Nondestructive Deflection Testing

G. R. RADA, M. W. WITCZAK, AND S. D. RABINOW

Two approaches for evaluating the structural capacity of asphalt concrete pavements from nondestructive deflection data are presented in the newly revised AASHTO Guide. Both procedures should ideally yield similar results, but studies to confirm this have not been performed. This paper describes a study undertaken by the authors to compare the two techniques. Deflection data from 1,049 tests performed on 55 homogeneous pavement sections were used. Structural capacities were calculated according to both AASHTO techniques in terms of the structural number (SN) value. On the basis of comparisons of the resulting SN values, it was concluded that both AASHTO techniques predict similar capacities. However, the computational time, required effort, and amount of information generated by each method are significantly different. Therefore, selection of the particular evaluation technique for use in a given project should be based on a clear understanding of the type of information required.

Since its introduction several decades ago, nondestructive deflection testing (NDT) has been an integral part of the structural evaluation of pavements. In the earliest years, this evaluation was based upon the analysis of a single deflection measurement resulting from a static or slow-moving load. However, as experience with deflection testing grew and technical advances were made, predictive capabilities greatly improved. Currently, the most accurate assessment of pavement structural capacity is achieved through the measurement and subsequent analysis of deflections at various radial distances (i.e., deflection basin) resulting from a dynamically applied load.

In the newly revised AASHTO Guide (*1*) for the design of pavement structures, two procedures for evaluating the effective structural capacity of an asphalt concrete pavement from nondestructive deflection data are presented: the Pavement Layer Moduli and the Direct Structural Capacity prediction techniques. Both approaches are based on the use of dynamic loads and the subsequent measurement of the deflection basin.

The first NDT approach utilizes the entire measured deflection basin to assess the in-situ modulus of each layer. The resulting moduli are then used, along with established AASHTO correlations between modulus and structural layer coefficient, to calculate the effective structural capacity of the pavement in terms of an effective structural number.

G. R. Rada and S. D. Rabinow, Pavement Consultancy Services, 4700 Berwyn House Road, #202, College Park, Md. 20740. M. W. Witczak, Department of Civil Engineering, University of Maryland, College Park, Md. 20740.

The second NDT approach is based on theoretical deflection equations that allow for prediction of the effective structural number (SN) directly from the maximum NDT deflection and knowledge of the subgrade modulus as interpreted from the outer geophone deflection measurements.

Both procedures should theoretically yield similar results, but, until now, verification studies have not been performed. This study is one of the first attempted direct comparisons in the United States and has been conducted primarily because of its importance to the long-range verification and modification of the NDT methodology suggested in the AASHTO Guide.

Three major research tasks were performed:

1. deflection and pavement data collection,
2. analysis of deflection data, and
3. comparison of results.

In Task 1, deflection basin data and other pertinent pavement information were collected for direct use in this study. Those data were analyzed using both AASHTO evaluation techniques in Task 2. And, in Task 3, a comparison of the effective structural capacity results generated was undertaken to verify the AASHTO NDT methodology.

A more detailed discussion of the study is presented in this paper. In the ensuing section, a brief description of the nondestructive testing equipment and a summary of the deflection data and pavement information collected are provided. A later section presents the analysis of deflection data according to the two AASHTO evaluation techniques. The results of the analysis are summarized and compared later. Finally, the major findings and conclusions of the study are discussed.

DEFLECTION AND PAVEMENT DATA COLLECTION

Nondestructive Testing Equipment

All nondestructive field data used in this comparison study were collected with a Phonix model ML10000 falling-weight deflectometer (FWD). This Phonix FWD model is a trailer-mounted pavement loading device capable of applying impulse loads ranging from approximately 2,500 lb to 24,000 lb. This impulse load range facilitates deflection studies on pavement structures ranging from low-volume roads to heavy-load airfield pavements.

The standard electronic package consists of six deflection sensors that can be positioned at various radial offset distances from the load plate center so that an accurate measurement of the complete deflection basin can be made under a given dynamic load. Additional standard features include a pavement surface and air temperature recording system and a trailer-mounted distance measuring instrument.

The complete FWD operation—data collection and subsequent data reduction and analysis—is accomplished using IBM-PC or compatible microcomputers and software systems developed by the authors. The FWD is operated by a single person from within the tow vehicle using a data collection program (COLLECT) that monitors the test mode condition and stores all pertinent field data such as load, deflections, and temperature.

Data reduction tasks are accomplished using the program REDUCE, which converts the raw field data from sequential test files to random-access binary files; allows for the correction of bad data elements and the creation of subset files and/or normalized deflection files; and provides tabular and graphical printouts of the deflection data along with statistical summaries. On completion, the resulting deflection data are analyzed using programs EMOD or SNEFF which back-calculate the in-situ layer moduli and/or structural capacity of the pavements tested.

Nondestructive Field Data

A total of 1,049 nondestructive deflection tests conducted between October 1985 and December 1986 were used in this study. These tests were performed on 55 unique pavement sections located in five different states: Virginia, Maryland, Colorado, Connecticut, and Texas.

In Virginia and Maryland, 593 tests on 23 pavement sections were conducted to assess the condition and structural capacity of the pavements under investigation and, on the basis of the results of the evaluation, to make rehabilitation recommendations. In Colorado, 253 tests results on 18 different pavement sections were used, along with other pertinent information, in the development of a data base for implementation of a pavement management system. And, in Connecticut and Texas, deflection tests were performed to demonstrate the operation and capabilities of the Phonix ML10000 FWD.

Table 1 is a summary of the pavement sections, indicating the section identification number, route number or name, location, pavement cross section, pavement temperature, and the number of tests conducted.

ANALYSIS OF NONDESTRUCTIVE DATA

In order to compare the approaches recommended in the AASHTO Guide detailing the uses of NDT within structural evaluation and rehabilitation studies, the deflection results for the pavements under investigation were analyzed using the EMOD and SNEFF programs. EMOD is a computerized solution to the Pavement Layer Moduli procedure recommended in the AASHTO Guide. SNEFF is the computerized solution to the AASHTO Direct Structural Capacity technique. Both programs and the methodology used in each are described below.

Subgrade Moduli Predictions

Regardless of the pavement structural evaluation technique selected, the first step in the overall analysis is to determine the in-situ subgrade modulus from the measured deflection basin. The fundamental concept used in either approach to establish this value is best illustrated in Figure 1, which shows a pavement structure being deflected under a dynamic NDT load. As the test is conducted, the load applied to the surface is distributed through the depth of the pavement system. The distribution of stresses, represented in this figure by the "Zone of Stress," is obviously dependent upon the stiffness or modulus of the material within each layer. As the stiffness of the material increases, the stress is spread over a much larger area.

More important, Figure 1 shows a radial distance ($r = a_{3e}$) in which the stress zone intersects the interface of the subbase and subgrade layers. When the deflection basin is measured, any surface deflections obtained at or beyond the a_{3e} value are due only to stresses, and hence deformations, within the subgrade itself. Thus, the outer readings of the deflection basin primarily reflect the in-situ modulus of the subgrade soil.

Using this concept, the in-situ subgrade modulus is determined in both EMOD and SNEFF programs from the composite moduli predicted for radial distances greater than the effective radius, a_{3e}, of the stress bulb at the pavement-subgrade interface, as indicated by the horizontal dashed line in Figure 2 for linear elastic subgrades or by the upward trend for nonlinear (stress dependent) subgrades. The composite modulus is a single-value representation of the overall pavement stiffness, at a given radial distance, that combines the modulus of elasticity of all layers present in the pavement.

The specific evaluation technique used by both programs involves the generation of pavement composite moduli plots from measured radial NDT deflections. Computer-generated plots of the composite moduli vs. radial distance are calculated by means of the following equations:

$$E_c = [2(1 - u_{sg}^2)p_c a_c]/\delta; \text{ if } r \leq 0.25*a_c \quad (1a)$$

or

$$E_c = \{[(1 - u_{sg}^2)p_c a_c]/\delta\}(C); \text{ if } r > 0.25*a_c \quad (1b)$$

where

E_c = composite modulus,
r = radial distance,
p_c = contact pressure applied by NDT device,
a_c = radius of contact of NDT device,
u_{sg} = Poisson's ratio of the subgrade,
δ = measured or predicted (from curve-fitting analysis) deflection, and
C = $[1.1*\log(r/a_c) + 1.15]$ or $[0.5*u_{sg} + 0.875]$ (lowest of the two values).

A more detailed discussion of the theories contained in this section is presented in the 1985 AASHTO Guide (*2*).

Pavement Layer Moduli Analysis

The AASHTO Pavement Layer Moduli analysis technique is based on the supposition that a unique set of layer moduli

TABLE 1 PAVEMENT TEST SECTIONS

SECTION ID NUMBER	ROUTE / LOCATION	PAVEMENT STRUCTURE LAYER 1	LAYER 2	LAYER 3	PAVEMENT TEMP.	NUMBER OF NDT POINTS
VADT5-2	Route 17 SBL, Stafford Co., Virginia	7.5" AC	6.0" GB	SG	73	9
VADT5-3	Route 3 EBL, Spotsylvania Co., Virginia	4.4" AC	6.0" GB	SG	76	19
VADT5-4	Route 301 NBL, King George Co., Virginia	9.0" AC	3.0" GB	SG	59	10
VADT5-5	Route 17 NBL, Caroline Co., Virginia	8.2" AC	7.0" GB	SG	54	46
VADT5-6	Route 17 NBL, Caroline Co., Virginia	5.8" AC	7.0" GB	SG	56	28
VADT5-9	Route 360 EBL, Richmond Co., Virginia	5.9" AC	6.0" GB	SG	52	46
VADT5-10	Route 203 SBL, Westmoreland Co., Virginia	3.1" AC	10.0" GB	SG	52	20
VADT5-11	Route 3 NBL, Lancaster Co., Virginia	5.3" AC	10.0" GB	SG	54	28
VADT5-12	Route 3 NBL, Lancaster Co., Virginia	4.4" AC	10.0" GB	SG	55	20
VADT5-13	Route 201Y NBL, Lancaster Co., Virginia	1.9" AC	6.0" GB	SG	60	8
VADT5-14	Route 200 NBL, Northumberland Co., Virginia	2.5" AC	10.0" GB	SG	58	25
VADT5-18	Route 14 EBL, King & Queen Co., Virginia	2.7" AC	8.0" GB	SG	80	11
VADT5-20	Route 360 WBL, King & Queen Co., Virginia	4.5" AC	6.0" CTB	SG	80	45
VADT5-21	Route 207 SBL, Caroline Co., Virginia	3.9" AC	6.0" CTB	SG	60	10
PAFB	Paine Street, Peterson AFB, Colorado	3.0" AC	6.0" GB	SG	65	15
PAFB-1	Hamilton Street, Peterson AFB, Colorado	2.5" AC	5.0" GB	SG	75	20
PAFB-2	Kincheloe Loop, Peterson AFB, Colorado	2.5" AC	5.0" GB	SG	80	10
PAFB-3	Thule Loop, Peterson AFB, Colorado	2.5" AC	5.0" GB	SG	90	13
PAFB-4	Suffolk Street, Peterson AFB, Colorado	2.5" AC	5.0" GB	SG	80	11
PAFB-5	Otis Street, Peterson AFB, Colorado	3.0" AC	5.0" GB	SG	90	19
PAFB-6	Mitchell Street, Peterson AFB, Colorado	2.0" AC	6.0" GB	SG	90	12
PAFB-7	Glasgow Street, Peterson AFB, Colorado	2.5" AC	5.0" GB	SG	90	9
PAFB-8	Loring Street, Peterson AFB, Colorado	2.5" AC	6.0" GB	SG	90	9
PAFB-9	Dover Ave., Peterson AFB, Colorado	2.5" AC	6.0" GB	SG	90	8
PAFB-10	Vincent Street, Peterson AFB, Colorado	2.5" AC	5.0" GB	SG	90	17
PAFB-11	ENT Ave., Peterson AFB, Colorado	2.5" AC	3.0" GB	SG	90	18
PAFB-12	Peterson Blvd., Peterson AFB, Colorado	4.5" AC	5.0" GB	SG	50	28
PAFB-13	Stewart Ave., Peterson AFB, Colorado	3.0" AC	5.0" GB	SG	65	31
PAFB-14	Truax Street, Peterson AFB, Colorado	3.0" AC	1.0" GB	SG	75	12
PAFB-15	Tinker Street, Peterson AFB, Colorado	2.5" AC	5.0" GB	SG	75	4
PAFB-16	Goodfellow Rd., Peterson AFB, Colorado	2.5" AC	6.0" GB	SG	75	10
PAFB-17	Duluth Street, Peterson AFB, Colorado	2.5" AC	5.0" GB	SG	80	7
VADT6-3	Route 29 NBL, Culpeper Co., Virginia	9.7" AC	6.0" GB	SG	88	34
VADT6-4	Route 55 WBL, Fauquier Co., Virginia	3.1" AC	12.0" GB	SG	79	13
VADT6-5	Route 29 SBL, Fauquier Co., Virginia	8.4" AC	6.0" GB	SG	74	25
VADT6-7	Route 17 SBL, Fauquier Co., Virginia	8.0" AC	3.0" GB	SG	87	53
CTDT-A6	Route 77 NBL, Guilford, Connecticut	4.0" AC	2.0" GB	SG	59	20
CTDT-B1	Route 218 EBL, Bloomfield, Connecticut	4.0" AC	29.0" GB	SG	54	20
CTDT-C8A	Route 80 EBL, Guilford, Connecticut	4.0" AC	3.0" GB	SG	55	11
CTDT-E4	Route 68 EBL, Wallingford, Conneticut	9.0" AC	10.0" GB	SG	44	14
CTDT-E7	Route 187 NBL, Bloomfield, Conneticut	9.0" AC	20.0" GB	SG	46	18
CTDT-F4	Route 202 NBL, New Hartford, Conneticut	4.3" AC	13.0" GB	SG	56	19
CTDT-F9	Route 140 EBL, Windsor Locks, Connecticut	3.3" AC	9.0" GB	SG	58	20
ARE-9A	Route 71 EBL, Lagrange, Texas	10.5" AC	12.0" GB	SG	91	12
ARE-10	Route 71 EBL, Lagrange, Texas	10.5" AC	12.0" GB	SG	93	12
ARE-11	Route 71 EBL, Lagrange, Texas	10.5" AC	12.0" GB	SG	96	12
ARE-12	Loop 360 SBL, Austin, Texas	3.0" AC	15.0" GB	SG	100	12
ARE-12A	Loop 360 SBL, Austin, Texas	3.0" AC	15.0" GB	SG	91	12
ARE-14	Route 183 NBL, Austin, Texas	2.5" AC	17.0" GB	SG	86	12
ARE-14B	Route 183 NBL, Austin, Texas	2.5" AC	17.0" GB	SG	103	9
ALF-F4Z	FHWA Turner-Fairbanks Research Lab, Virginia	5.0" AC	5.0" GB	SG	72	7
ALF-S10L1	FHWA Turner-Fairbanks Research Lab, Virginia	5.0" AC	5.0" GB	SG	58	18
ALF-F3Z	FHWA Turner-Fairbanks Research Lab, Virginia	7.0" AC	12.0" GB	SG	65	26
ALF-S10L2	FHWA Turner-Fairbanks Research Lab, Virginia	7.0" AC	12.0" GB	SG	59	32
CTI-GP	Grosvenor Pk. Loop Rd., Montgomery Co., MD	4.0" AC	6.0" GB	SG	60	60

Total Number of Sections = 55
Total Number of Test Points = 1049

AC = Asphalt Concrete Layer
CTB = Cement Treated Base Layer
GB - Granular Base Layer

exists such that the theoretically predicted deflection basin is equivalent to the measured deflection basin. This NDT approach utilizes the entire measured deflection basin to assess the in-situ (E_i) modulus of each layer. By using AASHTO correlations between the modulus and structural layer coefficient (a_i) values, the effective structural number of the pavement can be computed, assuming that the thicknesses of each layer (h_i) have been accurately determined.

The EMOD program has been developed to estimate in-situ pavement layer moduli from measured NDT deflection basin data. The analysis technique is based on the concepts of linear multilayer elastic theory and uses the Chevron N-Layer computer code (*3*) as a subroutine within the back-calculation procedure. In general, layer moduli are estimated from the combination of E_i values that result in the minimum cumulative residual error at all deflection (geo-

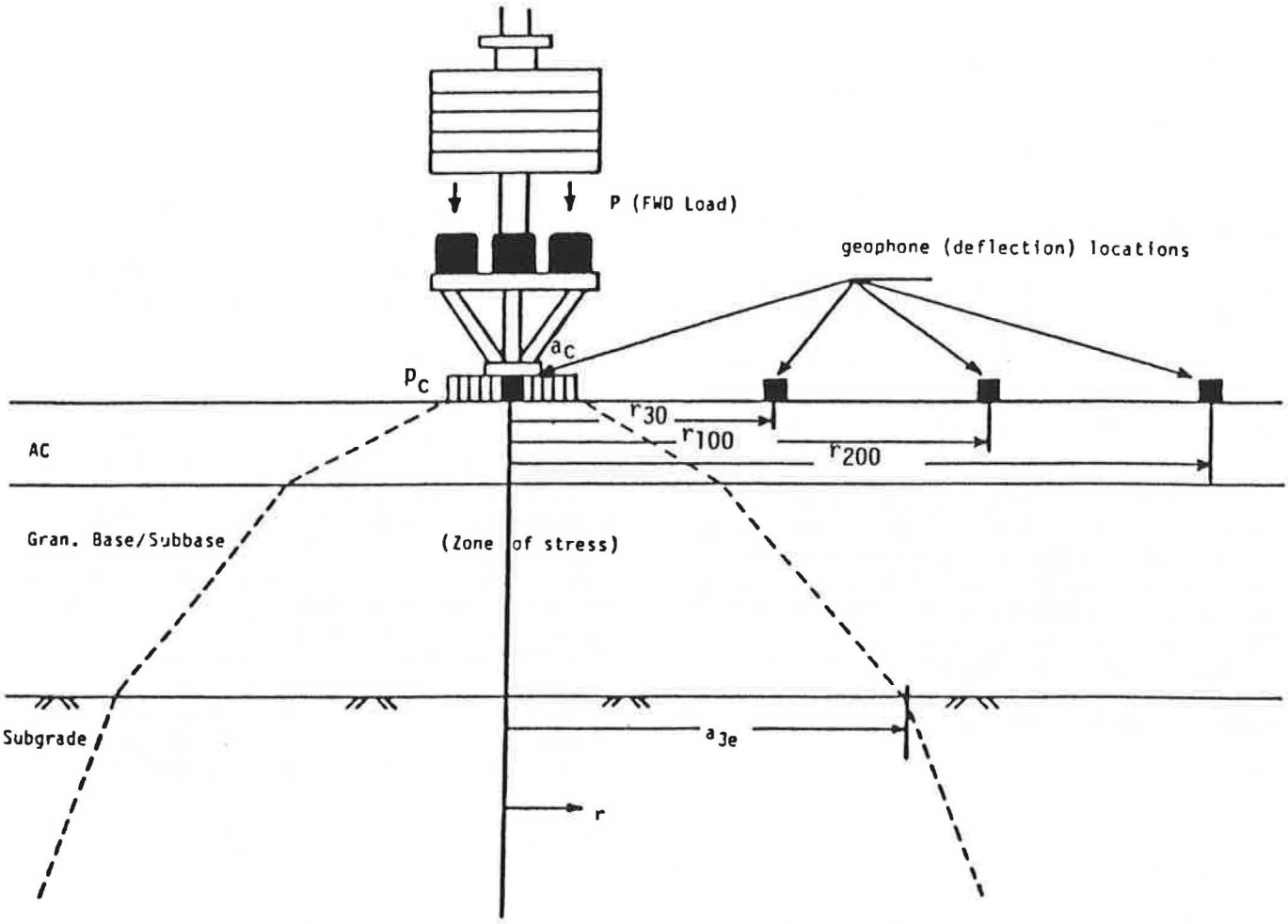

FIGURE 1 Schematic of stress zone within pavement structure under FWD load (*1*).

phone) readings. In order to utilize this program, the layer thicknesses and Poisson's ratio of each layer must be known or assumed.

Once the layer moduli have been calculated, the predicted asphalt concrete modulus must be corrected to a standard temperature of 68° to 78°F. The same temperature correction correlation recommended in the AASHTO Guide is contained in EMOD:

$$E(70) = \frac{E(T)}{10^{3.245 \times 10^{-4}*(2079.446 - T_p{}^{1.798})}} \quad (2)$$

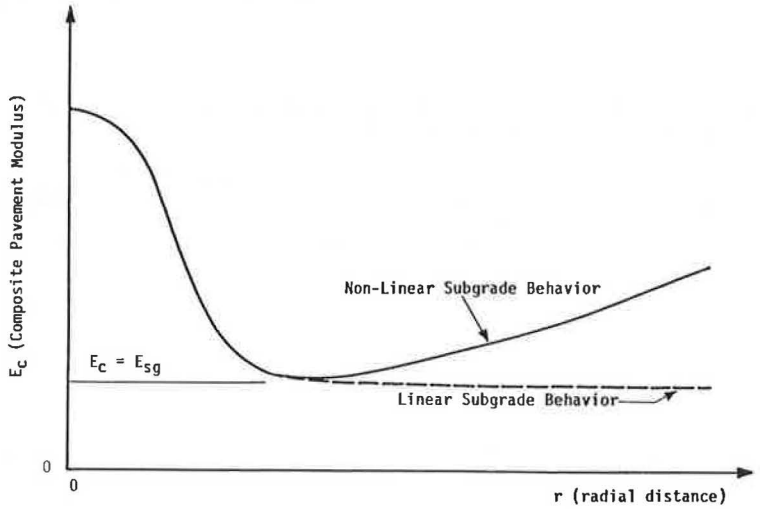

FIGURE 2 Composite modulus vs. radial distance plot.

where

$E(70)$ = temperature-corrected modulus,
$E(T)$ = modulus back-calculated from deflection basin (in EMOD), and
T_p = pavement temperature at time of NDT test.

After temperature correction, the estimated layer moduli are correlated with the empirical AASHTO structural layer coefficients through the use of nomographs or layer coefficient-modulus relations found in the AASHTO Guide. The predicted layer coefficients are then used, along with the known layer thicknesses, to estimate the effective structural capacity of the pavement system by means of the following expression:

$$SN = a_i h_i + a_2 h_2 + \ldots a_{n-1} h_{n-1} = \sum_{i=1}^{n-1} a_i h_i \quad (3)$$

However, instead of the nomographs or layer coefficient relations found in the AASHTO Guide, an alternate analytical form of layer coefficients to elastic modulus was used in this study. The theoretical bases behind the development of this alternate correlation are detailed in the 1985 AASHTO Guide (*2*) and are summarized below.

Assuming that the individual pavement layers (h_i, a_i) can be represented by equivalent thicknesses ($h_{s,i}$) of a standard material (a_s) having the same structural number, then

$$a_i h_i = a_i h_{s,i} \quad (4a)$$

or

$$a_i = a_s(h_{s,i}/h_i) \quad (4b)$$

Also, if the structural number of the equivalent layers is the same as that of the in-situ layers, then the "stiffness" of the two must be the same:

$$\frac{E_i h_i^3}{12(1 - u_i^2)} = \frac{E_s h_{si}^3}{12(1 - u_s^2)} \quad (5a)$$

or

$$\frac{h_{si}}{h_i} = \left[\frac{E_i(1 - u_s^2)}{E_s(1 - u_i^2)}\right]^{1/3} \quad (5b)$$

where

a_i = layer coefficient of i^{th} layer material,
a_s = layer coefficient of standard (arbitrarily selected) material,
E_i = elastic modulus of i^{th} layer materials,
E_s = elastic modulus of standard material,
u_i = Poisson's ratio of i^{th} layer material, and
u_s = Poisson's ratio of standard material.

Substituting Equation 5 into Equation 4 yields the alternate modulus-layer coefficient relation used in the study:

$$a_i = a_s\left[\frac{E_i(1 - u_s^2)}{E_s(1 - u_i^2)}\right]^{1/3} \quad (6)$$

This alternate relation fits with every material-layer-type correlation in the AASHTO Guide except for the asphalt surface course. To illustrate this fact numerically, if one arbitrarily selects (as was done in this study) a crushed stone base course as the standard material—$a_s = 0.14$, $E_s = 30{,}000$ psi, and $u_s = 0.35$—the computed a_i values shown in Table 2 are obtained for commonly accepted moduli values. As can be seen from this table, the predicted layer coefficients fit the AASHTO correlations very well except for the asphalt surface material.

Furthermore, if crushed stone is assumed to be the standard material, substitution of Equation 6 into Equation 3 yields the SN predictive equation contained in the EMOD program:

$$SN = \sum_{i=1}^{n-1} a_i h_i = \sum_{i=1}^{n-1} a_s\left[\frac{E_i(1 - u_s^2)}{E_s(1 - u_i^2)}\right]^{1/3} h_i$$

$$SN = 0.0043 \sum_{i=1}^{n-1} h_i \left(\frac{E_i}{1 - u_i^2}\right)^{1/3} \quad (7)$$

In addition to the above theoretical considerations, a much longer computational time is associated with the Pavement Layer Moduli technique because layer elastic solutions (e.g., Chevron) are required to iteratively back-calculate the layer moduli. However, since individual layer strengths are predicted, the results of the analysis can be used in the identification of problem layers/materials or as input into the more rational mechanistic approaches presently available.

TABLE 2 COMPARISON OF STRUCTURAL LAYER COEFFICIENTS FROM AASHTO AND ALTERNATE APPROACH

Material Type	Modulus (ksi)	Layer Coefficients	
		AASHTO	Alternate Approach
A.C. Surface	930	>.45	.44
	450	.44	.35
A.C. Base	340	.30	.31
Granular Base	30	.14	.14
Granular Subbase	15	.11	.11

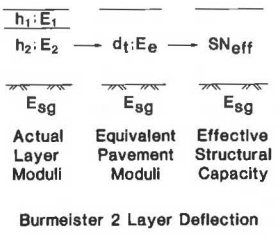

FIGURE 3 Basis for Direct Structural Capacity technique.

Direct Structural Capacity Analysis

The approach used in the AASHTO Direct Structural Capacity analysis technique is based on the premise that the overall pavement structural capacity is the result of the combined stiffness influence of each layer. Consequently, the maximum NDT deflection may be viewed as comprising two separate components: (1) pavement structural capacity and (2) subgrade support.

Using these concepts, a computerized solution (SNEFF) to the AASHTO Direct Structural Capacity analysis technique was developed. The procedure uses outer deflection basin data to estimate the subgrade modulus and then uses this parameter, along with the maximum NDT deflection, to directly estimate the effective structural capacity of the pavement system.

More specifically, the effective structural capacity of the pavement is determined in the program SNEFF through an iterative process. Assuming that the pavement structure can be represented by a one-layer system resting on the subgrade (see Figure 3) and that crushed stone ($a_s = 0.14$, $E_s = 30{,}000$ psi, and $u_s = 0.35$) is the standard material, the equivalent modulus (E_e) of the one-layer system (for a given iteration of the SN value) can be calculated by rearranging Equation 7 as follows:

$$E_e = (\mathrm{SN}/0.0043{*}h_t)^3(1 - u_{ie}^2) \tag{8}$$

where h_t is the total pavement thickness (i.e., $h_t = \Sigma h_i$).

In turn, the theoretical maximum deflection (δ_o) of the one-layer system with modulus E_e can be derived from the following expression contained in the 1985 AASHTO Guide (*2*):

$$\delta_o = \frac{2p_c a_c (1 - u_{sg}^2)}{E_{sg}} F_w$$

$$F_w = \frac{E_{sg}(1 - u_e^2)}{E_e(1 - u_{sg}^2)} + F_b\left(1 - \frac{E_{sg}}{E_e}\right)$$

$$F_b = [(1 + A^2)^{1/2} - A] \times \left[1 + \frac{A}{2(1 - u_{sg})(1 + A^2)^{1/2}}\right]$$

$$A = h_e/a_c$$

$$h_e = 0.9\, h_t \left[\frac{E_e(1 - u_{sg}^2)}{E_{sg}(1 - u_e)}\right]^{1/3} \tag{9}$$

where

F_w = Burmeister's two-layer deflection factor,
F_b = Boussinesq's one-layer deflection factor,
h_e = transformed thickness of pavement in terms of the subgrade modulus,
A = depth radii of the transformed section,
E_{sg} = subgrade modulus, and
u_e = Poisson's ratio of transformed section.

Therefore, by iterating on the SN value, the structural number that results in a predicted maximum deflection equal to, or within 1 percent of, the measured value is determined in the SNEFF program.

It should also be noted that the maximum measured NDT deflection must be adjusted to the standard temperature of 70°F before the effective structural number, SN, is calculated. The adjustment correlation used in SNEFF is that developed by the U.S. Army Corps of Engineers (*4*):

$$d_c = d_m/(1 + t_{ac}{*}m)$$

$$m = -8.491 \times 10^{-2} + (1.213 \times 10^{-3}){*}T_{air} \tag{10}$$

where

d_c = corrected maximum deflection (to 70° F),
d_m = measured maximum NDT deflection,
t_{ac} = total thickness of asphalt layers, and
T_{air} = air temperature at time of NDT test.

Because a simpler, two-layer solution is used in the Direct Structural Capacity technique, the computational time associated with this procedure is much faster. However, it cannot be used to isolate problem layers nor can the results be used as input into a mechanistic analysis.

Analysis Results

As previously described, calculations were performed analyzing the structural response of more than 1,000 sets of deflection measurements by means of Pavement Layer Moduli (EMOD program) and Direct Structural Capacity (SNEFF program) techniques. It should be emphasized that the calculations were performed for each set of deflection measurements individually, and that statistical analyses were performed on the results for each homogeneous pavement section investigated.

Table 3 presents the results of these analyses. Under the heading "EMOD ANALYSIS," reported results are based on the Pavement Layer Moduli techniques. Since all pavements were modeled as three-layer systems, results consist of mean layer moduli for the surface and base courses, as well as for the subgrade. The fourth column of this group represents the mean calculated effective SN value represented by the layer moduli.

Under the heading "SNEFF ANALYSIS," reported results are based on the Direct Structural Capacity techniques. The results include the mean subgrade modulus, thickness of pavement modeled, mean equivalent modulus of that thickness of pavement, and the mean calculated effective SN of that combination of modulus and thickness.

TABLE 3 STATISTICAL SUMMARY OF LAYER MODULI AND SN VALUES

	EMOD ANALYSIS				SNEF ANALYSIS			
SECTION ID NUMBER	MEAN LAYER MODULI (ksi) SURFACE	BASE	SUBGRADE	MEAN EFFECTIVE SN	MEAN SUBGRADE MODULUS (ksi)	PAVEMENT THICK. (in)	EQUIVALENT MODULUS (ksi)	MEAN EFFECTIVE SN
VADT5-2	445.8	42.2	20.0	3.52	20.0	13.5	192.3	3.50
VADT5-3	416.5	49.2	26.0	2.47	26.0	10.4	135.6	2.40
VADT5-4	305.9	36.0	23.6	3.18	23.6	12.0	209.3	3.20
VADT5-5	167.5	19.7	21.6	2.89	21.6	15.2	89.2	3.05
VADT5-6	214.5	28.6	15.3	2.53	15.3	12.8	87.3	2.55
VADT5-9	118.1	18.2	12.5	2.02	12.5	11.9	56.4	2.05
VADT5-10	179.9	33.8	18.5	2.25	18.5	13.1	55.9	2.25
VADT5-11	233.3	24.1	17.8	2.77	17.8	15.3	71.3	2.85
VADT5-12	323.9	32.4	23.6	2.80	23.6	14.4	85.6	2.85
VADT5-13	162.4	27.1	10.2	1.28	10.2	7.9	43.7	1.25
VADT5-14	856.6	21.8	16.8	2.33	16.8	12.5	56.2	2.15
VADT5-18	495.3	22.6	20.0	1.98	20.0	10.7	57.0	1.85
VADT5-20	490.7	93.3	21.1	2.83	21.1	10.5	198.2	2.75
VADT5-21	269.3	580.0	40.8	3.39	40.8	9.9	390.5	3.25
PAFB	585.5	51.0	17.5	2.13	17.5	9.0	121.1	2.00
PAFB-1	1080.4	61.5	21.4	2.05	21.4	7.5	165.6	1.85
PAFB-2	1138.7	65.0	18.9	2.08	18.9	7.5	165.6	1.85
PAFB-3	953.8	70.4	22.7	2.04	22.7	7.5	165.6	1.85
PAFB-4	469.1	52.3	15.2	1.72	15.2	7.5	107.2	1.60
PAFB-5	772.8	46.1	16.8	2.05	16.8	8.0	136.5	1.85
PAFB-6	929.5	63.3	17.8	1.96	17.8	8.0	125.7	1.80
PAFB-7	620.5	65.6	16.1	1.87	16.1	7.5	140.2	1.75
PAFB-8	1155.7	50.6	17.7	2.18	17.7	8.5	133.3	1.95
PAFB-9	739.1	61.9	17.2	2.09	17.2	8.5	133.3	1.95
PAFB-10	613.0	48.8	17.0	1.78	17.0	7.5	117.5	1.65
PAFB-11	1573.4	74.7	19.3	1.88	19.3	5.5	271.7	1.60
PAFB-12	348.2	62.5	21.0	2.32	21.0	9.5	146.6	2.25
PAFB-13	545.8	52.1	16.6	1.95	16.6	8.0	104.8	1.80
PAFB-14	1667.0	43.0	19.2	1.76	19.2	4.0	642.2	1.55
PAFB-15	153.7	20.0	10.3	1.22	10.3	7.5	39.8	1.15
PAFB-16	380.3	43.0	21.7	1.76	21.7	8.5	88.3	1.70
PAFB-17	1271.9	45.9	18.8	2.03	18.8	7.5	140.2	1.75
VADT6-3	327.8	16.8	21.4	3.71	21.4	15.7	156.5	3.80
VADT6-4	527.3	39.8	29.4	2.98	29.4	15.1	82.3	2.95
VADT6-5	971.0	46.2	37.5	4.72	37.5	14.4	383.7	4.70
VADT6-7	405.4	18.2	19.4	3.02	19.4	11.0	213.9	2.95
CTDT-A6	305.7	32.3	12.7	1.50	12.7	6.0	140.2	1.40
CTDT-B1	512.9	30.8	21.2	5.54	21.2	33.0	69.7	6.10
CTDT-C8A	578.6	50.0	21.0	2.00	21.0	7.0	203.7	1.85
CTDT-E4	516.6	29.6	34.3	4.65	34.3	19.0	195.2	4.95
CTDT-E7	475.1	39.7	23.8	6.24	23.8	29.0	162.0	7.10
CTDT-F4	591.3	24.2	45.9	3.32	45.9	17.3	83.8	3.40
CTDT-F9	769.8	34.3	14.8	2.68	14.8	12.3	98.3	2.55
ARE-9A	571.5	30.0	36.1	5.61	36.1	22.5	225.4	6.15
ARE-10	471.2	18.3	31.5	5.11	31.5	22.5	174.8	5.65
ARE-11	427.5	15.8	22.2	4.92	22.2	22.5	152.6	5.40
ARE-12	1559.0	107.1	125.7	4.78	125.7	18.0	209.3	4.80
ARE-12A	1516.9	103.8	122.7	4.73	122.7	18.0	202.8	4.75
ARE-14	653.3	42.1	18.9	3.64	18.9	19.5	72.4	3.65
ARE-14B	1236.4	44.4	17.9	3.92	17.9	19.5	88.3	3.90
ALF-F4Z	204.7	7.4	7.2	1.77	7.2	10.0	49.6	1.65
ALF-S10L1	338.9	11.8	8.3	2.08	8.3	10.0	81.8	1.95
ALF-F3Z	325.1	22.6	19.0	3.70	19.0	19.0	99.2	3.95
ALF-S10L2	398.5	33.9	18.8	4.07	18.8	19.0	127.9	4.30
CTI-GP	375.9	24.1	13.0	2.08	13.0	10.0	81.8	1.95

COMPARISON OF STRUCTURAL EVALUATION TECHNIQUES

The analysis results generated by the EMOD and SNEFF programs allowed for a direct comparison of the NDT structural evaluation techniques presented in the newly revised AASHTO Manual. As noted earlier, this study was conducted primarily because of its potential importance to the long-range verification and modification of the NDT methodology suggested in the AASHTO guide for asphalt concrete pavements.

The effective structural number for all 55 pavement sections under investigation has already been presented for the Pavement Layer Moduli approach (EMOD based) and the Direct Structural Capacity approach (SNEFF based) in Table 3. EMOD vs. SNEFF plots of the predicted effective SN values for *all* test points (1,049) and the *section means* are presented in Figures 4 and 5, respectively.

On the basis of these results, it is apparent that the effective structural capacities predicted by both AASHTO procedures are generally in excellent agreement with each other. The *R*-squared value (R = correlation coefficient) for both the point-by-point and section-by-section comparison is 0.98, and the

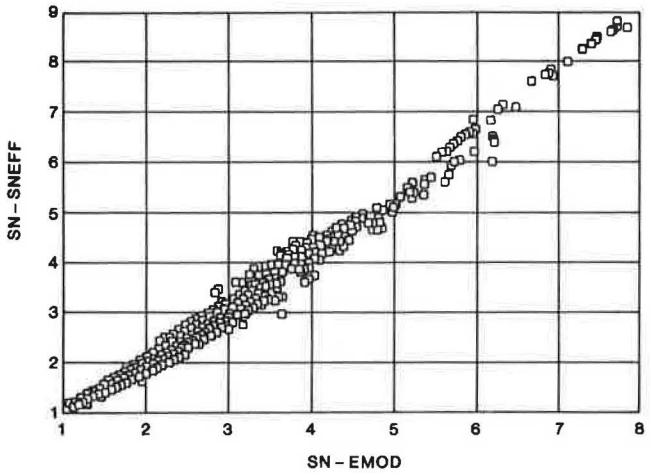

FIGURE 4 EMOD vs. SNEFF-predicted SN values for all test points.

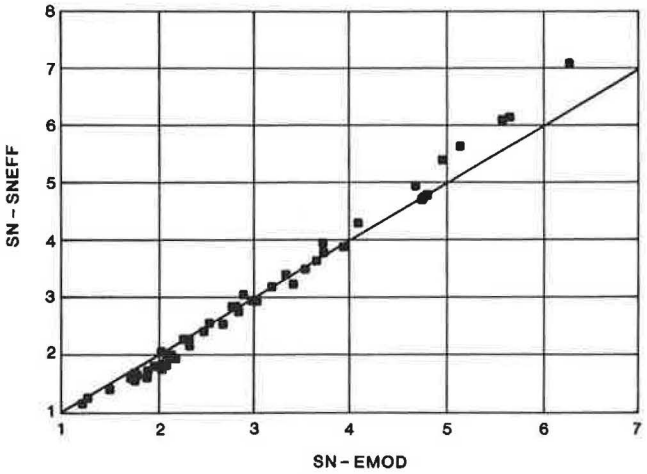

FIGURE 5 EMOD vs. SNEFF-predicted SN values for section means.

slope is approximately equal to one when the correlations are forced through a y-intercept of zero.

Figures 4 and 5 also show that for SN values approximately equal to or greater than 5, a more systematic error away from the line of equality occurs; the SNEFF program predicts larger SN values. However, because this systematic error is limited to 5 of the 55 pavement sections or 78 of the 1,049 test points investigated, further research is needed to compare the two AASHTO techniques for pavements with high SN values.

To further verify the agreement shown in Figures 4 and 5, a statistical comparison of the predicted SN values was undertaken. The acceptance criteria used to determine whether or not the hypothesis that the mean SN values generated by both AASHTO techniques are equal for the various pavement sections is shown in Table 4. The statistical test assumes that the SN values are normally distributed and that the true standard deviations are known.

Using the equations shown in Table 4, the test statistic (U) was calculated. The resulting values are summarized in Table 5. Next, assuming α values of 5 and 1 percent (or confidence levels of 95 and 99 percent) and using a two-sided confidence test yields $K_{\alpha/2}$ values of 1.96 and 2.57, respectively.

On the basis of the results presented in Table 5, acceptance of the hypothesis is dependent on the level of confidence selected. For an α value of 5.0 percent, 45 (or 81.8 percent) of the 55 pavement sections have equal means. On the other hand, for an α value of 1.0 percent, 50 (or 90.1 percent) of the pavement sections have statistically equal mean SN values.

TABLE 4 EQUATIONS FOR HYPOTHESIS TEST FOR EQUALITY OF SN MEANS (H: $u_x = u_y$)

Test Description:

Mean, two populations, known standard deviation

Test Statistic:

$$U = \frac{(\bar{x} - \bar{y})}{[(\sigma_x^2/n_x) + (\sigma_y^2/n_y)]^{1/2}}$$

where:
- U = test statistic (normal distribution)
- $\bar{x}$, $\bar{y}$ = mean of population x and y;
- σ_x, σ_y = standard deviation associated with population x and y; and
- n_x, n_y = number of units in population x and y.

Acceptance Criteria:

$$-K_{\alpha/2} \leq U \leq +K_{\alpha/2}$$

where:
- $K_{\alpha/2}$ = values of the standard normal variate with cumulative probability levels ($\alpha/2$) and ($1 - \alpha/2$).

Note: in this study, σ_x^2 and σ_y^2 represent the pooled variance of SN derived from the layer moduli and direct capacity approaches, respectively.

TABLE 5 RESULTS OF HYPOTHESIS TEST FOR EQUALITY OF SN MEANS

SECTION ID NUMBER	NUMBER OF NDT POINTS	EFFECTIVE SN METHOD 1 SN	METHOD 1 STD DEV	METHOD 2 SN	METHOD 2 STD DEV	PERCENT DIFFERENCE	U	STATISTICAL COMP. ACCEPTANCE ALPHA=5%	ALPHA=1%
VADT5-2	9	3.52	0.61	3.50	0.59	0.7%	0.12	YES	YES
VADT5-3	19	2.47	0.35	2.40	0.32	2.9%	0.59	YES	YES
VADT5-4	10	3.18	0.77	3.20	0.72	-0.6%	-0.12	YES	YES
VADT5-5	46	2.89	0.64	3.05	0.60	-5.6%	-2.09	NO	YES
VADT5-6	28	2.53	0.53	2.55	0.51	-0.8%	-0.20	YES	YES
VADT5-9	46	2.02	0.43	2.05	0.38	-1.7%	-0.39	YES	YES
VADT5-10	20	2.25	0.34	2.25	0.18	-0.2%	0.00	YES	YES
VADT5-11	28	2.77	0.43	2.85	0.42	-2.8%	-0.81	YES	YES
VADT5-12	20	2.80	0.50	2.85	0.50	-1.8%	-0.43	YES	YES
VADT5-13	8	1.28	0.23	1.25	0.18	2.3%	0.16	YES	YES
VADT5-14	25	2.33	0.20	2.15	0.20	7.7%	1.73	YES	YES
VADT5-18	11	1.98	0.12	1.85	0.13	6.7%	0.83	YES	YES
VADT5-20	45	2.83	0.32	2.75	0.31	2.7%	1.03	YES	YES
VADT5-21	10	3.39	0.45	3.25	0.32	4.2%	0.85	YES	YES
PAFB	15	2.13	0.29	2.00	0.24	6.3%	0.97	YES	YES
PAFB-1	20	2.05	0.30	1.85	0.18	9.6%	1.72	YES	YES
PAFB-2	10	2.08	0.24	1.85	0.14	11.2%	1.40	YES	YES
PAFB-3	13	2.04	0.11	1.85	0.09	9.3%	1.32	YES	YES
PAFB-4	11	1.72	0.13	1.60	0.14	6.9%	0.77	YES	YES
PAFB-5	19	2.05	0.18	1.85	0.18	9.7%	1.68	YES	YES
PAFB-6	12	1.96	0.13	1.80	0.10	8.1%	1.07	YES	YES
PAFB-7	9	1.87	0.11	1.75	0.09	6.4%	0.69	YES	YES
PAFB-8	9	2.18	0.21	1.95	0.15	10.7%	1.33	YES	YES
PAFB-9	8	2.09	0.15	1.95	0.15	6.6%	0.76	YES	YES
PAFB-10	17	1.78	0.16	1.65	0.17	7.4%	1.03	YES	YES
PAFB-11	18	1.88	0.22	1.60	0.15	14.9%	2.29	NO	YES
PAFB-12	28	2.32	0.40	2.25	0.32	3.1%	0.71	YES	YES
PAFB-13	31	1.95	0.24	1.80	0.19	7.6%	1.61	YES	YES
PAFB-14	12	1.76	0.12	1.55	0.10	12.0%	1.40	YES	YES
PAFB-15	4	1.22	0.06	1.15	0.05	5.4%	0.27	YES	YES
PAFB-16	10	1.76	0.21	1.70	0.22	3.6%	0.37	YES	YES
PAFB-17	7	2.03	0.27	1.75	0.18	13.7%	1.43	YES	YES
VADT6-3	34	3.71	0.37	3.80	0.37	-2.5%	-1.01	YES	YES
VADT6-4	13	2.98	0.24	2.95	0.25	0.9%	0.21	YES	YES
VADT6-5	25	4.72	0.91	4.70	0.91	0.4%	0.19	YES	YES
VADT6-7	53	3.02	0.35	2.95	0.34	2.5%	0.98	YES	YES
CTDT-A6	20	1.50	0.26	1.40	0.21	6.8%	0.86	YES	YES
CTDT-B1	20	5.54	0.24	6.10	0.27	-10.1%	-4.82	NO	NO
CTDT-C8A	11	2.00	0.24	1.85	0.17	7.5%	0.96	YES	YES
CTDT-E4	14	4.65	0.50	4.95	0.48	-6.5%	-2.16	NO	YES
CTDT-E7	18	6.24	0.53	7.10	0.58	-13.8%	-7.02	NO	NO
CTDT-F4	19	3.32	0.36	3.40	0.34	-2.4%	-0.67	YES	YES
CTDT-F9	20	2.68	0.21	2.55	0.17	4.9%	1.12	YES	YES
ARE-9A	12	5.61	0.20	6.15	0.16	-9.7%	-3.60	NO	NO
ARE-10	12	5.11	0.13	5.65	0.15	-10.6%	-3.60	NO	NO
ARE-11	12	4.92	0.19	5.40	0.22	-9.7%	-3.20	NO	NO
ARE-12	12	4.78	0.13	4.80	0.12	-0.4%	-0.13	YES	YES
ARE-12A	12	4.73	0.18	4.75	0.18	-0.4%	-0.13	YES	YES
ARE-14	12	3.64	0.13	3.65	0.09	-0.2%	-0.07	YES	YES
ARE-14B	9	3.92	0.11	3.90	0.07	0.6%	0.12	YES	YES
ALF-F4Z	7	1.77	0.08	1.65	0.06	6.7%	0.61	YES	YES
ALF-S10L1	18	2.08	0.17	1.95	0.14	6.5%	1.06	YES	YES
ALF-F3Z	26	3.70	0.32	3.95	0.35	-6.8%	-2.45	NO	YES
ALF-S10L2	32	4.07	0.50	4.30	0.25	-5.6%	-2.50	NO	YES
CTI-GP	60	2.08	0.42	1.95	0.40	6.4%	1.94	YES	YES

In either case, the results show that from a statistical point of view the SN values predicted by both AASHTO methods are in excellent agreement. This is particularly true for pavements with SN values less than 5.

Finally, a comparison of NDT-derived vs. typical SN values was performed. Typical SN values were calculated using Equation 4. The layer thicknesses for input into this equation have been summarized in Table 1. Typical structural layer coefficients were assumed for the various materials as follows:

a_i = 0.42 for asphalt concrete surfaces up to a maximum thickness of 3 in. For thicknesses greater than 3 in., a value of a_i = 0.28 (typical of asphalt concrete base materials) was assumed.

a_i = 0.24 for cement-treated bases.

a_i = 0.14 for granular base materials.

The resulting NDT-derived (average of values shown in Table 3) and typical SN values are presented in Table 6 and plotted in Figure 6. On the basis of these results, a very good correlation (R-squared = 0.86) between the NDT-derived and typical SN values exists. Also, the NDT-derived SN values appear to be quite reasonable.

TABLE 6 NDT-DERIVED VS. TYPICAL SN VALUES

SECTION ID NUMBER	NUMBER OF NDT POINT	AVG NDT SN VALUE	TYPICAL SN VALUE	% DIFF
VADT5-2	9	3.5	3.3	6.0%
VADT5-3	19	2.4	2.4	1.4%
VADT5-4	10	3.2	3.3	-3.4%
VADT5-5	46	3.0	3.6	-21.2%
VADT5-6	28	2.5	3.0	-18.1%
VADT5-9	46	2.0	2.9	-42.5%
VADT5-10	20	2.3	2.6	-15.6%
VADT5-11	28	2.8	3.2	-13.9%
VADT5-12	20	2.8	3.0	-6.2%
VADT5-13	8	1.3	1.6	-26.5%
VADT5-14	25	2.2	2.4	-7.1%
VADT5-18	11	1.9	2.2	-14.9%
VADT5-20	45	2.8	2.5	10.4%
VADT5-21	10	3.3	2.3	30.7%
PAFB	15	2.1	2.0	3.1%
PAFB-1	20	2.0	1.7	12.8%
PAFB-2	10	2.0	1.7	13.5%
PAFB-3	13	1.9	1.7	12.6%
PAFB-4	11	1.7	1.7	-2.4%
PAFB-5	19	2.0	1.9	2.6%
PAFB-6	12	1.9	1.6	14.9%
PAFB-7	9	1.8	1.7	6.1%
PAFB-8	9	2.1	1.8	12.8%
PAFB-9	8	2.0	1.8	10.9%
PAFB-10	17	1.7	1.7	0.9%
PAFB-11	18	1.7	1.4	19.5%
PAFB-12	28	2.3	2.3	-0.7%
PAFB-13	31	1.9	1.9	-1.3%
PAFB-14	12	1.7	1.4	15.4%
PAFB-15	4	1.2	1.7	-43.5%
PAFB-16	10	1.7	1.8	-4.0%
PAFB-17	7	1.9	1.7	10.1%
VADT6-3	34	3.8	3.9	-3.9%
VADT6-4	13	3.0	2.8	5.6%
VADT6-5	25	4.7	3.6	23.6%
VADT6-7	53	3.0	3.1	-3.9%
CTDT-A6	20	1.5	1.8	-24.1%
CTDT-B1	20	5.8	5.3	8.9%
CTDT-C8A	11	1.9	1.9	1.3%
CTDT-E4	14	4.8	4.2	12.5%
CTDT-E7	18	6.7	5.5	17.5%
CTDT-F4	19	3.4	3.3	1.8%
CTDT-F9	20	2.6	2.5	4.4%
ARE-9A	12	5.9	4.9	16.7%
ARE-10	12	5.4	4.9	8.9%
ARE-11	12	5.2	4.9	5.0%
ARE-12	12	4.8	3.2	33.2%
ARE-12A	12	4.7	3.2	32.5%
ARE-14	12	3.6	3.3	9.5%
ARE-14B	9	3.9	3.3	15.6%
ALF-F4Z	7	1.7	2.5	-46.2%
ALF-S10L1	18	2.0	2.5	-24.1%
ALF-F3Z	26	3.8	3.9	-2.0%
ALF-S10L2	32	4.2	3.9	6.8%
CTI-GP	60	2.0	2.3	-14.1%

SUMMARY AND CONCLUSIONS

The ultimate goal of this study was to compare the NDT structural evaluation techniques presented in the newly revised AASHTO Guide. In order to accomplish this objective, three major tasks were undertaken: (1) deflection and pavement data collection, (2) analysis of deflection data, and (3) comparison of analysis results.

In Task 1, a total of 1,049 deflection test results, along with other pertinent pavement information, performed on 55 unique pavement sections in five different states were collected. This information was analyzed in Task 2 using computerized solutions of the AASHTO NDT techniques. In Task 3, a detailed comparison of the analysis results was performed to verify the NDT methodologies contained in the new AASHTO Guide.

Based upon the results of this study, it was concluded that both AASHTO evaluation procedures predict similar structural capacities. This is particularly true for pavements with SN values of 5 or less. However, the computational time, required effort, and amount of information generated by each method are significantly different.

The Pavement Layer Moduli procedure is a slower solution,

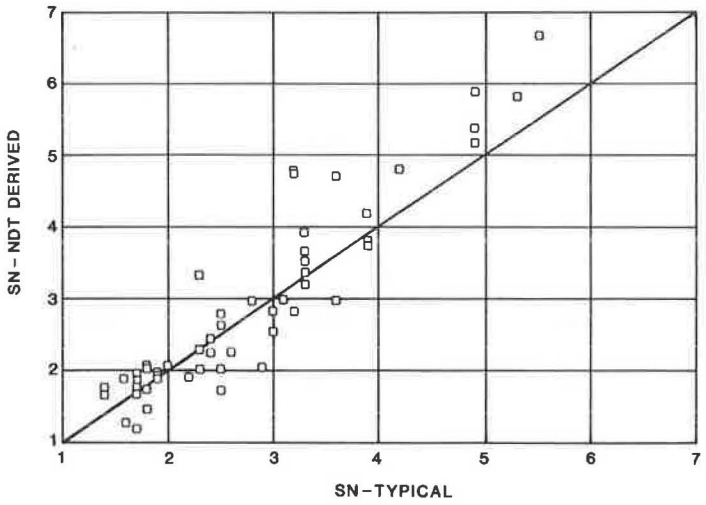

FIGURE 6 NDT-derived vs. typical SN values.

but the results of the analysis can be used in the identification of problem layers/materials or as input into the more rational mechanistic approaches presently available. The Direct Structural Capacity procedure, on the other hand, is a much faster computational solution but cannot be used to isolate problem layers, nor can the results be used as input into a mechanistic analysis. Therefore, although both procedures yield similar results, the selection of the particular AASHTO NDT evaluation technique for use in a given project should be based on a clear understanding of the type of information required.

REFERENCES

1. *AASHTO Guide for Design of Pavement Structure.* American Association of State Highway and Transportation Officials, Washington, D.C., 1986.
2. *Proposed AASHTO Guide for Design of Pavement Structures.* NCHRP Project 20-7/24. American Association of State Highway and Transportation Officials, Washington, D.C., 1985.
3. J. Michelow. *Analysis of Stresses and Displacement in an N-Layered Elastic System Under a Load Uniformly Distributed Over a Circular Area.* California Research Corporation, 1963.
4. A. J. Bush. *Nondestructive Testing for Light Aircraft Pavements.* Technical Report GL-80-1. U.S. Army Engineer Waterways Experiment Station, Vicksburg, Miss., 1980.

Publication of this paper sponsored by Committee on Flexible Pavement Design.